For submission to Canadian Journal of Fisheries and Aquatic Science (January 9, 2009)

Form and uncertainty in stock-recruitment relations: observations and implications for Atlantic salmon management

William S.C. Gurney*[1,2], Philip J. Bacon[2], Philip McGinnity[3], Julian Mclean[2], Gordon Smith[2] and Alan Youngson[2]

[1] *Department of Statistics and Modelling Science, University of Strathclyde, GLASGOW G1 1XH, Scotland*

[2] *Fisheries Research Services, Freshwater Laboratory, PITLOCHRY, Scotland.*

[3] *University of Cork, CORK, Ireland*

Abstract

This paper reports a series of investigations of stock-recruitment relations for Atlantic salmon which we believe have wider implications. We regard these relations as stochastic functions characterised by an expected stock-recruitment relation (ESR) and a process noise component representing deviations from this expectation driven by uncharacterised variability in the physical and biotic environment. We fit the ESR using non-linear least-squares minimisation and use simulation techniques to derive confidence limits. We find that the process noise is well represented by a negative binomial distribution with constant shape factor and mean proportional to the expected recruitment. Analysis of stock recruitment relations characterising various segments of the life-cycle of salmon from the Girnock Burn in N.E. Scotland reveals two independent regulatory processes, one between ova and fry and the other between fry and smolts, with the survival at sea being clearly density independent. Comparative studies of a group of Atlantic salmon stock recruitment relations for populations in Scotland, Ireland and Canada, together with a series of simulation studies reveals that low-stock sigmoidality is a potentially common characteristic of salmon ESR's. We demonstrate the critical effect this may have on extinction probability and hence on the choice and utilisation of ESR forms for precautionary management policy.

*Corresponding author

Introduction

Overview

The stock-recruitment paradigm dates from the pioneering work of Ricker (1954) and Beverton and Holt (1957). Despite evidence that some species have recruitment dynamics too subtle to be readily summarised by a one to one relationship with stock size (e.g. Roughgarden et al., 1988; Sakuramoto, 2005) this paradigm, together with the related idea of maximum sustainable yield (e.g. Clark, 1990), has been a mainstay of fisheries management for more than sixty years.

In many marine species, stock-recruitment observations are complicated by measurement error (Needle, 2002) and difficulties in defining stock and recruits (often for reasons of spatial or jurisdictional heterogeneity). For anadromous fishes (such as salmonids) who return to their natal catchment with considerable accuracy, both definitional and observational errors can be much smaller. However, even for salmonids in single large catchments, observed stock recruitment relations (e.g. Crozier and Kennedy, 1995) are typically very noisy.

In view of the prevalence of both measurement and definitional error, the central thrust of statistical work on stock-recruitment relations has been the use of Baysian methods to define how well the parameters of a group of chosen functional forms can be defined (e.g. Chen and Holtby, 2002; Schnute and Kronlund, 2002; Michielsens and McAllister, 2003), and the incorporation of environmental data (e.g. Chen and Irvine, 2001). In this paper we focus principally on a salmonid dataset in which definitional uncertainty and measurement error are both small and in which the remaining noise is process error associated with unknown variability in the physical and biotic environment. We follow Needle (2002) in arguing that this process noise will inevitably be large enough for the stock-recruitment relationship to be considered as intrinsically stochastic.

We are thus concerned both with the expected stock recruitment relation (formally the expected recruitment given stock abundance), and with the distribution and intensity of the process noise around this expected recruitment. This recruitment process noise combines with the process noise in the remaining (linear) part of the life-cycle to drive stochastic fluctations in stock abundance.

Even when the expected stock recruitment (ESR) relation and the expected marine survival (or, more generally, linear-phase survival) combine to produce a deterministically viable equilibrium, the fluctuations driven by variability in recruitment and survival can be large enough to produce a high probability of extinction, especially where the population exhibits an Allee effect (Chen et al., 2002). We show that at any given level of process noise, the mean time to extinction depends on the shape of the expected stock recruitment relation at both very low and very high stocks – areas in which data necessarily tends to be least available.

Our investigation shows that recruitment and linear-phase noise play distinct roles in stock-recruitment function identification– with linear-phase noise playing a positive role in allowing us to discern the ESR within an envelope of recruitment

process noise. These findings allow us to define 'stock' and 'recruits' so as to maximise the accuracy of our identification of the stock-recruitment relation. They also allow us to define ESR functions yielding 'worst-case' estimates of extinction time.

The data

A survey of Atlantic salmon stock-recruitment datasets in the N.E. Atlantic has been complied by Chaput et al. (2003). Data for many species including Atlantic salmon are given at *http://www.mscs.dal.ca/ myers/welcome.html*. The work reported here began with an extended investigation of the rich, long-term, dataset on Atlantic salmon from the Girnock Burn in N.E. Scotland, and was later extended to include a selection of other datasets for the same species, chosen to allow us to investigate key aspects of the stock-recruitment modelling process.

The ***Girnock Burn*** is a tributary of the River Dee in N.E. Scotland, whose spawning population of Atlantic salmon has been the subject of intenstive monitoring for over 40 years. The resulting dataset has been extensively described by Gurney et al. (2009) and references therein. It contains almost complete sequences of numbers of spawners (distinguished by sea-age, river-age and sex) and individuals emigrating down river to smolt (distinguished by age). It also contains partial sequences of fry abundance (from autumn electro-fishing), aged parr abundance (from electro-fishing and scale analysis) and parr growth performance (from mark recapture studies, see Bacon et al., 2005).

A resistive fish-counter has been operated at the Logie weir on the ***N.Esk***, in N.E. Scotland since 1981 and has yielded an acceptably accurate measure of potential spawners (Shearer, 1990). Numbers of aged smolts emigrating are estimate from a mark recapture process described by Chaput et al. (2003). Records of the estuarine and coastal catches are used to calculate yearly estimates of pre-fishery abundance.

An ova to smolt relation for the ***River Bush*** in Northern Ireland is described by Crozier and Kennedy (1995), who also give a relation between ova numbers and a semi-quantitative fry abundance index.

Locke and Mowbray (1995) describe an ova to fry stock recruitment relation for the ***Nepisiguit River***, New Brunswick, Eastern Canada. Fry abundance was assayed at 16 sites by electrofishing removal between barrier nets. Incoming spawners were counted using counting fences deployed from July to October and ova numbers were calculated from number of female spawners.

Chaput and Jones (1992) describe an exceptionally long (1947-1992) series of stock recruitment data for multi-sea-winter Atlantic salmon in the ***Margaree River*** in Nova Scotia, Eastern Canada. 'Stock' is defined as spawning escapement and recruits as returns to the river. Total returns were calculated as the sum of the commercial catch and in-river returns. In-river returns were estimated from angling catches, and escapement was defined as in-river returns minus angling catch.

Materials and Methods

Expected stock-recruitment curves

Most investigations of relations between the abundance of one stage in a population's life history (stock) and a later stage (recruits), centre on an an algebraic expression describing the expected recruitment ($\widehat{R}$) for a given value of stock abundance (S). In this investigation we shall use a number of forms for this expected stock-recruitment (ESR) relation.

The first of these is a humped form based on the widely used relation due to Ricker (1954), which we extend to allow positive curvature near the origin, by setting

$$\widehat{R} = \widehat{R}_{max} \left[\frac{S}{S_{max}} \right]^k \exp \left[k \left(1 - \frac{S}{S_{max}} \right) \right]. \tag{1}$$

In this extended Ricker (eRicker) form, $\widehat{R}_{max}$ represents the maximum possible expected recruitment, S_{max} represents the equivalent stock, and k is the sigmoidality parameter. If $k > 1$ then small stocks have reduced per-capita fecundity, and the ESR curve has positive curvature near the origin. If $k < 1$ then small stocks have enhanced per-capita fecundity, and the slope near the origin is larger than that given by the standard Ricker (sRicker) expression (equation 1 with $k = 1$).

Provided that we avoid unbiological negative values of the sigmoidality parameter, all variants of equation 1 predict that as stock rises, expected recruitment goes through a single maximum before proceeding asymptotically to zero. Although some data sets appear consistent with this paradigm, many are equally consistent with the supposition that as S becomes large, expected recruitment approaches a finite asymptote from below. Hence, we add to our candidate ESR curves, a version of the form proposed by Beverton and Holt (1957), adapted as described by Myers et al. (1995) and Myers (2001) to provide the possibility of positive curvature near the origin, thus

$$\widehat{R} = \widehat{R}_{max} \left[\frac{S^k}{S^k + S_h^k} \right] \tag{2}$$

In this extended Beverton-Holt (eBH) form, $\widehat{R}_{max}$ has the same interpretation as before, S_h is the stock at which $\widehat{R} = \widehat{R}_{max}/2$, and k is the sigmoidality parameter; with $k = 1$ leading to the standard Beverton-Holt (sBH) form, $k > 1$ implying positive curvature at the origin, and $k < 1$ implying enhanced per-capita fecundity at low stock.

A number of stock-recruitment datasets used to inform stock management show little sign of non-linearity. Thus we complete our set of candidate ESR curves with a group of linear and piece-wise linear forms. For a closed population we expect that the ESR curve should pass through the origin, so we define a

broken-stick (BS) form

$$\widehat{R} = \begin{cases} [\widehat{R}_{max}/S_b]S & \text{if } S < S_b \\ \widehat{R}_{max} & \text{otherwise.} \end{cases} \quad (3)$$

where $\widehat{R}_{max}$ has its usual interpretation and S_b is the stock abundance above which $\widehat{R} = \widehat{R}_{max}$. We note that if S_b becomes very large, equation 3 defines a straight line through the origin (the L1 form). For completeness, we also include an unconstrained straight line, which we call the L2 form, and write

$$\widehat{R} = \widehat{R_0} + \beta S. \quad (4)$$

where β is the fecundity and R_0 is the zero-stock recruitment.

Fitting stock-recruitment data

Early in this investigation we experimented with Markov-chain Monte-Carlo methods to estimate the posterior distribution of the stock-recruitment parameters given a specific set of observations. We found that reasonable choices of likelihood function often yielded implausibly precise posterior distributions, with characteristics depending sensitively on the presence or absence of 'influential points'. We concluded that a more robust approach would fit ESR curves using conventional non-linear minimisation and assess uncertainty by resampling from simulated data sets generated assuming that the best-fit ESR curve and the observed variability about it represent the underlying stochastic stock-recruitment function (see e.g. Davidson and Hinkley, 1997).

In the work reported here we fitted candidate ESR curves by minimising the sum of squared differences between observations and predictions using the Nelder-Meade non-linear optimisation algorithm implemented in the R routine 'optim'. A typical result, together with the correponding observations is shown in Fig. 1a.

Examination of the standardised residuals yielded by the fitting process normally suggests (as in Fig. 1c) that their standard deviation is independent of spawner numbers, implying that the (un-standardised) residuals at a given stock have a standard deviation proportional to the ESR for that stock. This supposition is supported by Fig. 1d, where we compare the observations to the one and two standard deviation contours implied by a standard deviation which is proportional to expected fry abundance.

To determine confidence limits for the fitted curves we generated a thousand (statistically equivalent) simulated data sets with points at the same spawner numbers as the observed dataset. Output at those spawner numbers was drawn from a normal distribution with mean equal to the best fit and standard deviation equal to the product of that mean with the overall standard deviation of the standardised residuals. We fitted each simulated dataset in the same way as the observations (see Appendix, Fig. A1) and then scanned the envelope of fitted

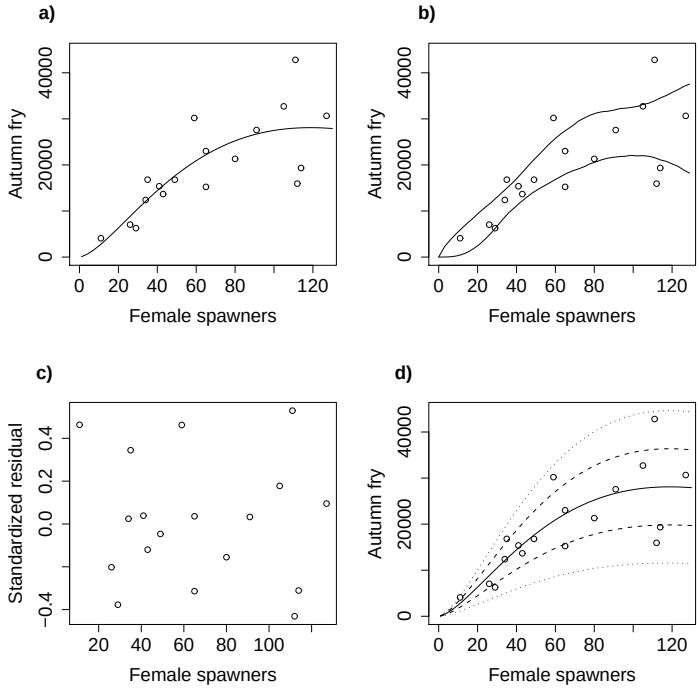

Figure 1: Fitting the Girnock Burn female spawner → autumn fry data with the extended Ricker model. a) shows observations (open circles) and the best fit expected stock recruitment curve (solid line, $R^2 = 0.617$). b) shows observations (open circles) and the 95% confidence limits (solid lines) for the ESR curve determined from 1000 simulated datasets – see text. c) shows the standardised residuals (s.d.=0.294) between the best fit ESR curve and the observations. d) illustrates the data, the best fit (solid line) and the 1 s.d.(dashed line) and 2 s.d.(dotted line) contours implied by the assumption of constant c.v. residuals.

ESR curves to find the 2.5% and 97.5% percentiles for each input value. A typical example of the resulting confidence limits is shown in Fig. 1b.

As a useful byproduct of this exercise, we obtain estimates for the distribution of the parameters which characterise the ESR relationship. As an example, Fig. 2 shows frequency plots and correlograms for the fitted values of the three parameters which define the eRicker form when fitted to the data in Fig. 1a.

These distributions frequently permit additional deductions about which characteristics of the observations can safely be regarded as generic. For example the results in Fig. 2 show that 70.9% of simulated datasets yield best fit ESR curves with noticeably sigmoidal form (which we, rather arbitrarily, identify with $k > 1.2$) and 39.9% yield ESR curves with a noticeably 'humped' shape (which we, again rather arbitrarily, identify as having a maximum at less than 83% of the maximum observed spawner abundance). They also show that the parameters R_{max} and S_{max} have bimodal distributions with the majority of the probability mass at values consistent with visual analysis of the observations,

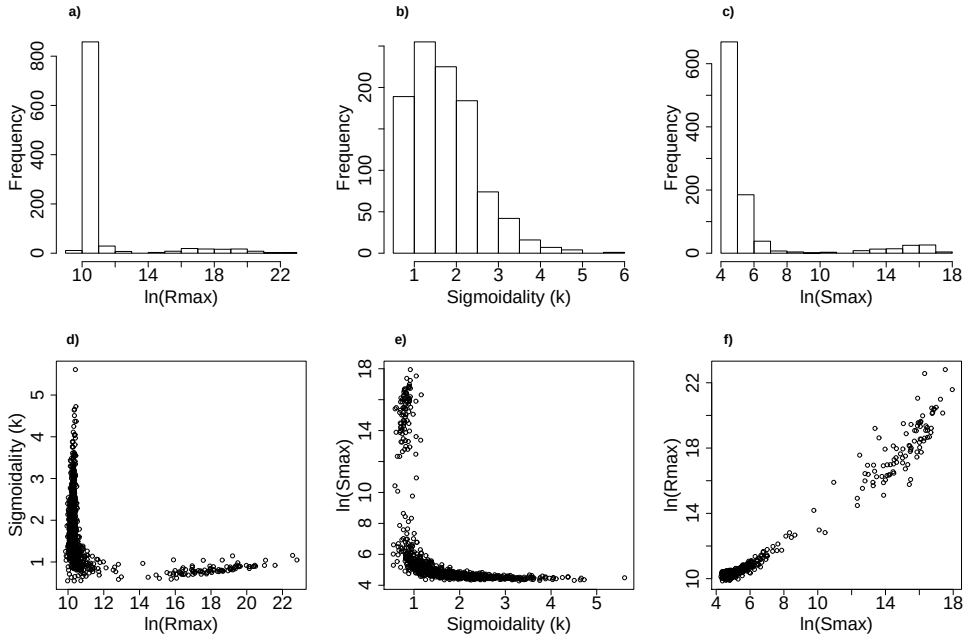

Figure 2: Parameter values and relationships for the simulated datasets used to calculate the 95% confidence limits in Fig. 1. a) shows a frequency histogram for $\ln(R_{max})$ implying that the great majority of the fitted values lie in the range $2.2 \times 10^4 \rightarrow 6.0 \times 10^4$, with a small subsidiary group in the range $1.2 \times 10^6 \rightarrow 4.8 \times 10^8$. b) shows a frequency histogram for the sigmoidality parameter k, which implies that 70% of simulated datasets have noticeably sigmoidal form ($k > 1.2$). c) shows a frequency histogram for $\ln(S_{max})$ which implies that 38% of the simulated datasets have $S_{max} < 0.83 \max(S_{obs})$, the majority of the simulated datasets have S_{max} in the range $55.6 \rightarrow 403$ with a subsidiary group in the range $1.3 \times 10^5 \rightarrow 6.5 \times 10^7$. d) to f) show correlograms for all pairwise combinations of the three fitted parameters.

accompanied by a very small subsidiary group in which these parameters have very large (functionally infinite) values.

Taken together these parameter distributions give strong support to the view that the stock recruitment observations in Fig. 1a imply an ESR curve which has positive curvature near the origin, and negative curvature at higher spawner numbers. However (as we might expect from visual examination) support for falling expected recruitment at very high spawner numbers is weak.

Strategic simulations

Even when data (e.g. Fig. 1a) allows reliable definition of the expected stock recruitment relation (ESR) there is considerable generation on generation variability around this curve. Any simulation which is to be useful for stock management purposes must characterize this variability. Since we have neither detailed knowledge of the underlying processes, nor information about their physical or biological drivers, we have little option but to regard them as random.

In the case of the Girnock trap data the counts of spawning females are com-

plete and thus essentially noise free. Although the accompanying fry abundance estimates are subject to considerable systematic error from the scale-up process, re-sampling calculations (J. Thorley, pers.comm.) showed this to be relatively consistent from year to year. The majority of observed variability around the ESR shown in Fig. 1a can thus be ascribed to process rather than observation error, so the required random function should have statistical properties close to those of the observed residuals. Specifically it should have a coefficient of variation which is independent of spawner numbers and whose value is close to that of the observed standardised residuals.

For consistency with the minimisation process used to determine the ESR, the dataset simulations from which we estimate confidence limits make the assumption that observations are normally distributed. For simulations of fry 'counts' with a minimum expected value in excess of 2000 and a coefficient of variation of 0.294, this assumption is relatively innocuous. However our strategic population simulations will need to encompass the possibility of extinction, so we need to adopt a characterisation of variability which is more plausible when spawner (and hence expected fry) numbers are small.

Since the fry numbers are counts, a natural null model would be a Poisson process. However for expectations in the range 2000-20000 a Poisson model would predict s.d.'s in the range 45-141, compared to observed values of 588-5880.

An obvious choice for modelling such an over-dispersed Poisson process is the negative binomial distribution, which, if it has mean λ and shape factor θ, predicts fluctuations around the mean with coefficient of variation c given by

$$c^2 = \frac{1}{\lambda} + \frac{1}{\theta}. \tag{5}$$

For λ in the range $2000 \rightarrow 20000$ and c in the range $0.1 \rightarrow 0.3$, this implies that to a very good approximation $c^2 \approx \theta^{-1}$. Hence we model the full (stochastic) stock recruitment relation by writing

$$R(S) = B_N(\widehat{R}(S), \theta) \tag{6}$$

where $\widehat{R}(S)$ is the best-fit expected stock recruitment relation (ESR) and B_N is a negative binomially distributed random variable with shape factor θ related to the standard deviation of the standardised residuals about the ESR.

Results

Models and observations

As an exemplary application in the previous section, we used the extended Ricker ESR form to fit data relating the number of female Atlantic salmon spawning in the Girnock Burn to the abundance of fry the following autumn. In this section we re-examine the same dataset using our remaining candidate ESR forms. The

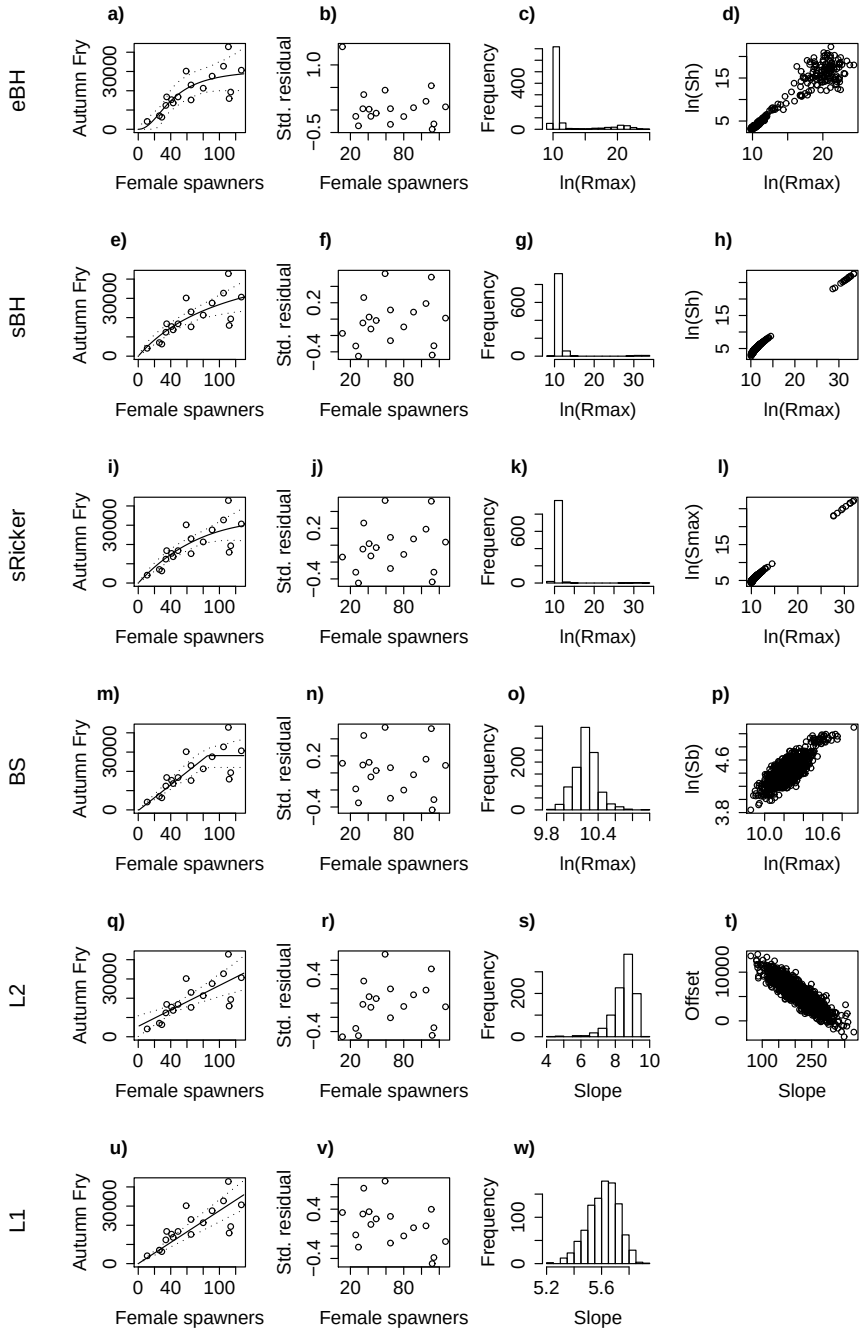

Figure 3: Fitting the Girnock Burn female spawner → autumn fry data with candidate ESR forms – eBH: row 1 (a → d), sBH: row 2 (e → h), sRicker: row3 (i → l), BS: row 4 (m → p), L2: row 5 (q → t), L1: row 6 (u → w). Column 1 (a,e,i,m,q,u) shows observations (circles), best fit ESR (solid) and 95% confidence limits (dotted). Col 2 shows std. residuals. Cols 3 and 4 show parameter distributions and correlations from simulated datasets.

Table 1: Fitting the Girnock Burn female spawner → autumn fry data with candidate ESR forms. Fit characteristics for fits shown in Fig. 3.

Form	R^2	Std. resid. s.d.	Simulation features
eRicker	0.617	0.29	70% $k > 1.2$, 38% $S_{max} > \max(S_{obs})$
eBH	0.618	0.43	80% $k > 1.2$
sBH	0.601	0.29	
sRicker	0.606	0.28	4% $S_{max} > \max(S_{obs})$
BS	0.602	0.29	
L2	0.563	0.33	
L1	0.498	0.35	

best fits are shown in Fig. 3 and the R^2 values, standardised residual properties and any notable features of the fit are given in Table.1.

The results for the non-linear ESR forms are shown in the upper four rows of Fig. 3, which illustrate fits with the extended Beverton Holt (eBH), the standard Beverton-Holt (sBH), the standard Ricker (sRicker) and broken stick (BS) forms. Comparing the eBH fit (Fig. 3 frames a → d) and the eRicker fit given in the last section (Figs. 1 and 2) shows that both offer considerable support for positive ESR curvature at low spawning stock. While the eRicker fit shows no obvious bias in the distribution of standardised residuals, the eBH fit undershoots the lowest stock observation, thus producing an obvious outlier in the standardized residuals which is almost solely responsible for their large standard deviation.

The sBH (frames e→h) and sRicker (frames i→l) forms produce best fit curves, confidence limits and standardized residual distributions which are essentially indistinguishable. Their standardised residual distributions are clearly biased, with residuals for stocks below 40 females being predominantly negative. In common with the eBH and eRicker fits, both exhibit a small group of simulated datasets with very large $\widehat{R}_{max}$ indicating data whose form is linear.

By contrast, the broken-stick (BS) form produces an equally plausible fit, with considerably less residual bias at low stocks and all simulated datasets showing finite $\widehat{R}_{max}$. This arises because the BS form can achieve a straight line through the data by setting $\widehat{R}_{max}$ greater than the largest observed value, whereas the curved forms must make $\widehat{R}_{max}$ very large to achieve the same effect.

For completeness, we have also fitted two linear forms – an unconstrained straight line (L2) and a straight line through the origin (L1). Both fits show evidence of bias in the residuals; negative at high and low stocks and positive between for the unconstrained line and a trend from positive towards negative for the straight line through the origin. In both cases the R^2 values are lower than those for the non-linear fits, with the L1 fit being the only one to explain less than 50% of the variance.

Our overall conclusions are that the Girnock data robustly indicates an expected stock recruitment curve which saturates at high stock and which has

positive curvature at low stock. The data give no robust support to the hypothesis that at high stocks, recruitment decreases with increasing stock.

Life-history stages and stock-recruitment relations in the Girnock Burn

Aside from the length of time over which it has been collected, and the consequent quantity of data it contains, the great power of the Girnock Burn dataset lies in contemporaneous counts of different life-history stages and careful age-determinations which allow us to allocate individuals to year classes. In this section of the paper we use this data richness to investigate the nature of the stock-recruit relationships between various way-points in the salmon life cycle.

We fit an extended Ricker (eRicker) ESR curve to each life-history segment and compare this best fit, together with 95% confidence limits, with the data (Fig. 4). In the same figure we show standardised residuals about the ESR and parameter distributions from the simulated datasets used to determine the 95% confidence limits. In Table 2 we summarise the properties of the best fits.

Table 2: Fitting life-cycle segments for Girnock Burn salmon. Fit characteristics for the fits illustrated in Fig. 4. Columns 8 and 9 show the percentage of simulated datasets which have visibly humped forms ($S_{max} < \max(S_{obs})$ and visibly knee'd forms ($k > 1.2$) respectively.

Stock	**Recruits**	$\boldsymbol{R^2}$	**Std. Resid.**	**Best Fit Parameters**			**Simulations**	
			s.d.	$\boldsymbol{R_{max}}$	$\boldsymbol{S_{max}}$	$\boldsymbol{k}$	Hump	Knee
Ova/10^4	Fry	0.621	0.29	28736	60.6	1.40	37%	62%
Females	Fry	0.617	0.29	28095	119	1.57	39%	74%
Females	Smolts	0.419	0.32	4146	101	0.87	74%	23%
Fry	Smolts	0.447	0.35	4794	40868	0.88	47%	34%
Females	Females	0.100	0.65	63.7	136	0.54	50%	19%
Smolts	Females	0.284	0.62	9.6×10^5	6.2×10^7	1.12	1%	44%

In the first two rows of Fig. 4 and Table 2 we show fits to the relation between the abundance of fry at the autumn fry survey and the number of ova which produce them (frames a→d) or the number of adult females who produced the ova (frames e→h). Since the count of adult females makes no differentiation between grilse and multi-sea-winter salmon it comes as little surprise to observe that the ova→fry relation has marginally more predictive power than that for spawner→fry. However, both fits tell essentially the same story, namely that there is a strongly density-dependent process occuring between ova deposition and late autumn fry abundance whose expectation explains some 61% of the year to year variation in fry recruitment, with the residual variability (standardised residual c.v. 29%) being mainly attributable to year on year process variation.

Frames (m→p) of Fig, 4 show the relation between autumn fry abundance and the resulting numbers of emigrants to sea (smolts – who, of course, emigrate at a

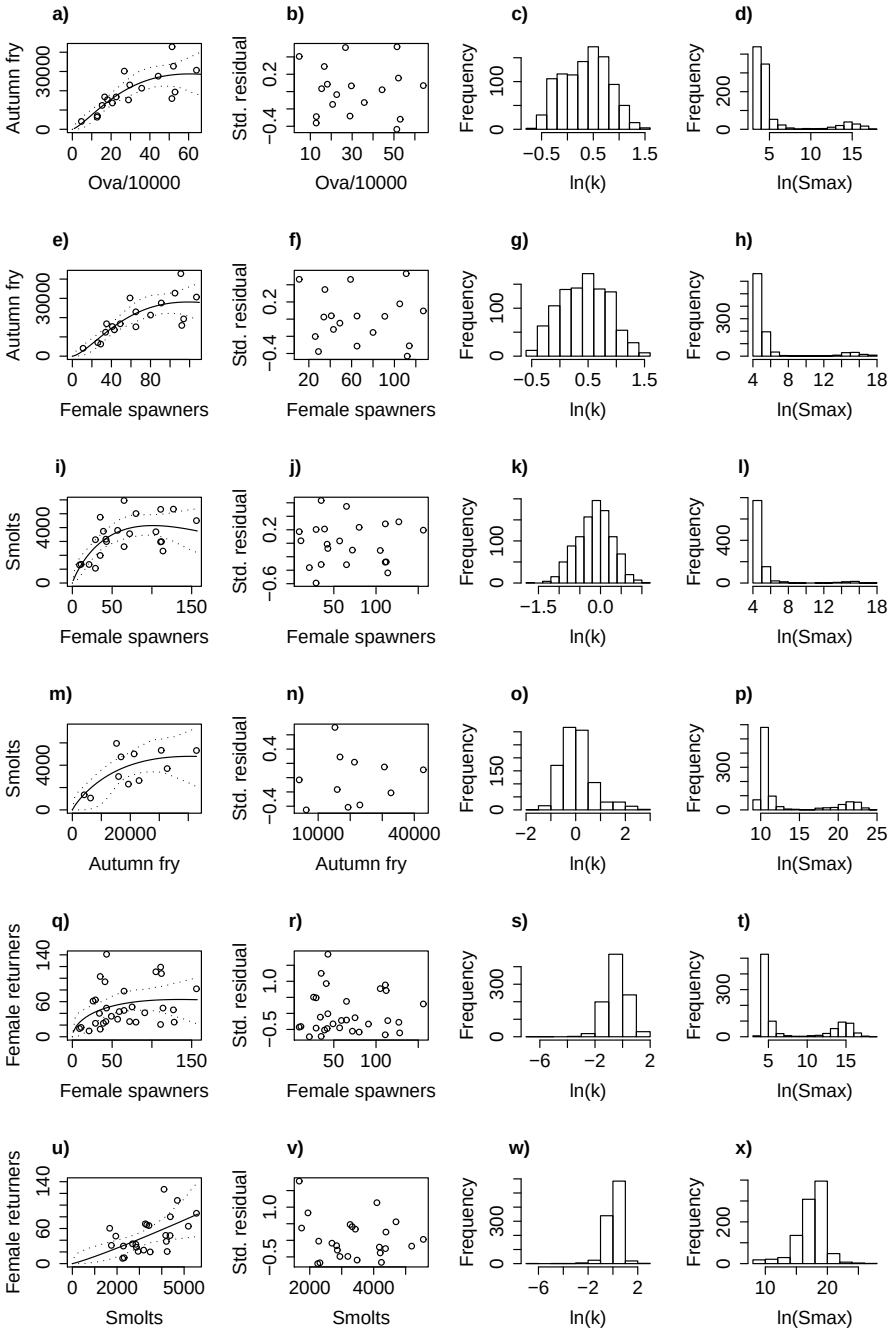

Figure 4: Fitting life-cycle segments for Girnock Burn salmon. Col. 1 (a,e,i,m,q) shows data (circles), best fit eRicker ESR (solid) and 95% confidence limits (dotted). Col 2 shows standardized residuals. Cols 3 and 4 show parameter frequency plots from simulated data. Row 1 (a→d): ova (estimated) → autumn fry. Row 2 (e→h): female spawners → autumn fry. Row 3 (i→l): female spawners → smolts. Row 4 (m→p): autumn fry → smolts. Row 5 (q→t): female spawners → female returners. Row 6 (u→x): smolts → female returners.

range of ages). Again we see a clearly non-linear ESR, although its explanatory power (45%) is rather less than the ova→fry case, and the year on year process variation consequently higher (standardised residual c.v. 35%). This implies that a second distinct density dependent process operates on the parr stage of the lifecycle.

The serial combination of density dependence at the fry and parr stages clearly underlies the observed relation between spawner and smolt numbers (Fig 4 i→l), whose form, explanatory power and standardised residual c.v. closely resemble that of the fry→parr relation displayed in frames (m→p). For future reference, we note that although the best fit form of both fry→smolt and spawner→smolt ESR relations has no sigmoidal (knee'd) character (i.e. $k < 1.2$), some 25% of simulated datasets yield a sigmoidal ESR and consequently the lower side of the 95% confidence envelope is noticeably sigmoidal.

The bottom row of Fig. 4 (frames u→x) show the relationship between stock at the beginning of the sea-phase of the life-cycle (smolts) and recruits at its end (females returning spawn). For consistency we have fitted this data with the eRicker form, but the results confirm what is evident from eye-balling the data and simple linear regression; namely that this relation shows very considerable year on year (process) variability but no discernably non-linearity. This confirms that no density dependent processes operate on the sea-phase of the life-cycle.

Careful examination of the standardised residuals for the smolt→returner fit demonstrates that although we can plausibly assume that the residual c.v. is independent of stock size, the distribution of these residuals is significantly right-skewed. The same phenomenon can be observed in the spawners→returners relation shown in frames (q→t), which has a non-linearity inherited from the spawner to smolt relation (frames i→l) subsumed within it, almost buried behind the intense, right-skewed, noise of sea-survival variation.

The conclusions from this stage of our investigation are simple and clear. Density dependence within the salmon life-cycle occurs only in the juvenile riverine stages (fry and parr) with marine survival showing high (and right skewed) density independent variability. Within the riverine phase two distinct density dependent proceses operate, one on the ova→fry transition (i.e. on fry) and the other on the fry→smolt transition (i.e. on parr). The second of these shows considerably more variability than the first.

Salmon stock-recruitment relations in Scotland, Ireland and Canada

In this section we compare the stock-recruitment relations observed for Atlantic salmon at various sites in eastern Scotland, Ireland and Atlantic Canada with those for the Girnock Burn population discussed above. Three of the data sets use ova numbers (estimated from female spawning stock) as their input ('stock') and two of those use smolt numbers as output ('recruits'). For purposes of comparison we have evaluated the ova to smolt relationship for the Girnock population.

For consistency with our earlier treatment of the Girnock Burn data we have

fitted each data set with an eRicker expected stock recruitment curve (ESR). In general we performed the least squares minimisation without constraints on the parameters other than that they take positive values, but in the case of the two N. Esk datasets (for which the most parsimonious statistical model is a horizontal straight line) we have constrained the sigmodiality parameter $k \geq 1$ to avoid numerical problems associated with $k \to 0$. We show the fits, 95% confidence limits, standardised residuals and parameter distributions from the simulated data sets used to evaluate confidence limits in Fig. 5. We give the achieved R^2, the standardised residual c.v., the best fit parameters and the proportion of the simulated data sets used to evaluate confidence limits which visible maxima and sigmodiality (Table 3).

Table 3: Salmon stock-recruit relations from sites in Scotland and Canada. Fit characteristics for fits shown in Fig. 5. Column 4 shows standardised residual c.v. Columns 8 and 9 show the percentage of simulated datasets which have visibly humped forms ($S_{max} < \max(S_{obs})$ and visibly knee'd forms ($k > 1.2$) respectively.

Site	**Relation**	$\boldsymbol{R^2}$	**Resid.**	**Best Fit Parameters**			**Simulations**	
			s.d.	$\boldsymbol{R_{max}}$	$\boldsymbol{S_{max}}$	$\boldsymbol{k}$	Hump	Knee
Nepisiguit	ova→fry	0.318	0.56	21.75	87.9	1.67	92%	79%
Girnock	ova→smolt	0.423	0.31	4183	50.1	0.77	75%	12%
Bush	ova→smolt	0.227	0.33	25997	243	1.83	99%	80%
N. Esk	ova→smolt	0.0012	0.18	1.7×10^5	804	0.1	67%	1%
N. Esk	adult→adult	0.015	0.20	21953	3890	0.1	83%	23%
Margaree	adult→adult	0.275	0.33	4459	3914	0.44	55%	0%

One of the benefits of the kind of comparative study reported here is that we can look for common features of ESR form. For example, although two of the data sets shown in Fig. 5 (Girnock ova→smolt, and Margaree spawner→returner) show no evidence of low-stock sigmoidality, the majority of fits either show sigmoidal best fit ESR's (the Nepisiguit and the Bush), or have low stock confidence envelopes whose shape or width prevent our ruling out such sigmoidality (both N. Esk data sets). We further note that in no case does the distribution of the standardised residuals show any obvious pattern – thus supporting a model of underlying process noise with a (system specific) coefficient of variation which is independent of spawning stock size.

Comparing the fit qualities † given in Table 3 with the spawning stock ranges and maximum recruitments shown in Fig. 5 reveals a clear correlation between

†In the case of the data from the River Bush we note that the achieved value of R^2 (0.227) compares poorly with the value (0.422) reported by Crozier and Kennedy (1995) when fitting the same data with a standard Ricker form. We have refitted this data using the same form (not shown) and find $R^2 = 0.183$, which is very close to the value which would result if Crozier and Kennedy had reported a value of $R = 0.422$ (which is much more commensurate with the visual appearance of the data) as R^2.

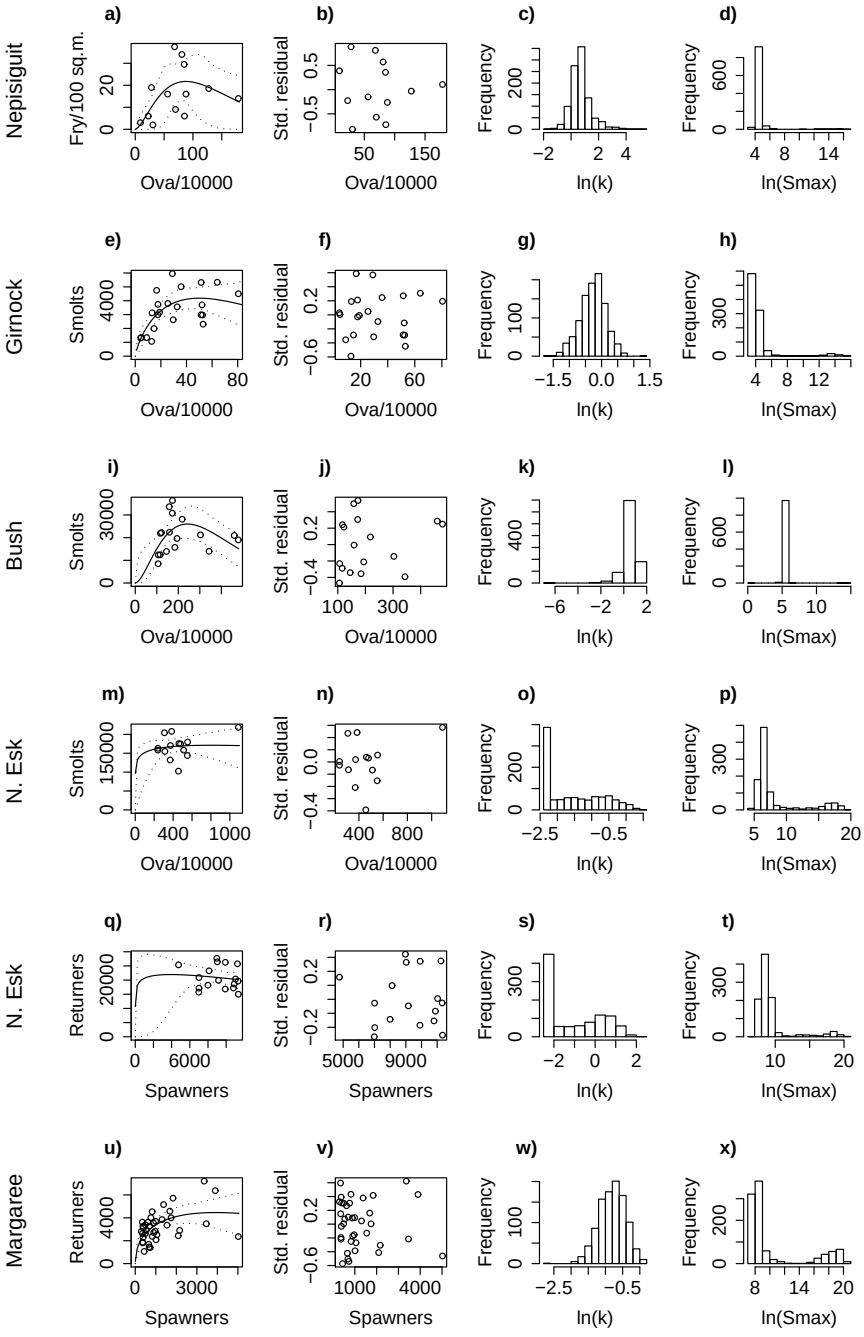

Figure 5: Salmon stock-recruitment relations from Scotland, Ireland and Canada. Col. 1 (a,e,i,m,q) shows data (circles), best fit eRicker ESR (solid) and 95% conf. lims. (dotted). Col 2 shows std. resid. Cols 3 and 4 show frequency plots from simulated data. Sites: Nepisiguit River (N.B.), ova→fry: row 1(a→d); Girnock Burn, ova→smolts: row 2(e→h); River Bush, ova→smolts: row 3(i→l); North Esk, ova→smolts: row 4(m→p); North Esk, spawners→pre-fishery returns: row 5(q→t); Margaree River (N.S.), spawners→returners: row 6(u→x).

large spawning population, low achieved R^2 , and low standardised residual standard deviation. We shall argue below that this correlation arises because physically large systems frequently exhibit systematic environmental heterogeneity, implying (region or site specific) heterogeneity in the competitive processes underlying the stock-recruitment function.

Temporal stability of expected stock recruitment relations

A frequently posed question in regard to stock-recruitment relations is whether the processes which produce them are in a statistical sense stationary over time. Unfortunately, most such relationships are deduced from runs of data whose overall length is barely adequate to allow any underlying relationship between stock and expected recruitment to be visible through the combination of process noise and measurement error. Subdividing such data sets in an effort to detect long term trends in the ESR is thus unrewarding.

However, several of the data sets used in this investigation are long enough for it to be possible to divide the time series into two parts and still obtain an adequately defined ESR for each part. We show (Fig. 6) the results of such an

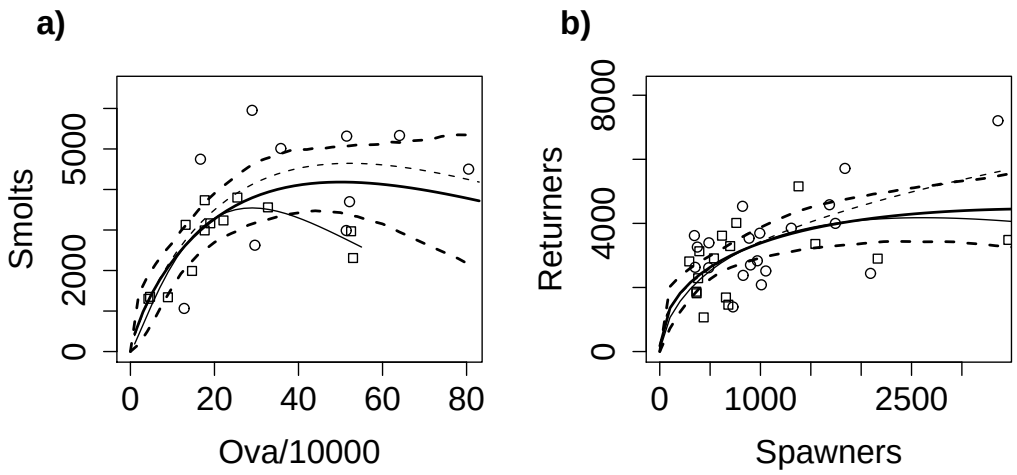

Figure 6: Temporal stability of stock recruit relations in a) the Girnock Burn and b) the Margaree River. The points show observations, circles show early years (1967-1976 in the Girnock and 1947-1972 in the Margaree) and squares show late years (1977-1999 in the Girnock and 1973-1990 in the Margaree). The heavy line shows the best fit ESR for the data as a whole, with the equivalent 95% confidence intervals shown by heavy dashed lines. The best fit ESR for the early data is shown by a light dashed line and for the later data by a light solid line.

exercise on Atlantic salmon data from the Girnock Burn, in eastern Scotland, and the Margaree River in eastern Canada. In each frame of this figure we use different symbols for the early and late parts of the time-series. We plot the

best fit ESR determined from the whole data set together with the equivalent 95% confidence limits, and also the best fit ESR's determined from each of the sub-sets.

In the Girnock Burn dataset we can see that the decadal trend in spawner numbers described by Gurney et al. (2009) results in stock data from the early year subset clustering preferentially in the range $3 \times 10^5 \rightarrow 8 \times 10^5$ ova, while the data from the later year subset cluster below 3×10^5 ova. None the less, the best fit ESR for the early year subset is everywhere comfortably within the 95% confidence range for the curve fit to the data as a whole, and the best fit ESR for the later year subset only emerges from the whole data 95% confidence envelope for stocks in between 4×10^5 and 5×10^5 ova, as a result of two apparent outliers (1981 and 1989) both being contained in the later year subset.

For the Margaree data the situation is simpler. The data from both subsets is similarly distributed across the range of spawners and the ESR from both sub sets lies almost entirely within the 95% confidence range of the whole data ESR; the only exception being the early years subset whose ESR just crosses the upper boundary of the 95% confidence envelope for stocks in excess of 3000 spawners. We thus conclude that for neither data set can we reject the null hypothesis that the expected stock-recruitment relation is time independent.

Stock-recruitment identification in a noisy environment

It is clear from the observations reported above that even in the most favourable circumstances the relationship between stock and recruitment will exhibit considerable noise. While some of this may be measurement error, much is due to variation in the underlying biology driven by unknown or unquantified physical or biotic factors. In this paper we regard this 'process noise' as part of the stock recruitment relation. However, since we cannot characterised it independently, its presence forms a significant obstacle to accurate identification of the expected stock recruitment relation (ESR). Moreover, in the real world the observations from which such an identification may be made will necessarily span a relatively short time period (typically a few tens of years) and be complicated by (unrelated) environmental noise in the linear phase of the life-cycle

In this section we report a series of numerical experiments designed to determine how effectively we can identify the underlying regularity of the stock-recruitment relation (specifically its expected stock-recruitment curve and the intensity of the process noise around it) in the presence of noise in both the linear and the non-linear parts of the life-cycle.

A single population

We first investigate identification of the ESR for a single population. To simulate the observations from which we shall attempt to reconstruct the ESR we assume that we are observing a population of a semelparous organism charaterised by a

stock recruitment function $R(S)$ whose expected value for a given stock, $\widehat{R}(S)$, is given by a standard Ricker function (equation 1 with $k = 1$), with process noise about that expected value being negative binomially distributed with shape parameter θ_R. Thus if the stock at generation g is S_g, the resulting recruitment R_g is

$$R_g = B_N(\widehat{R}(S_g), \theta_R). \tag{7}$$

where $B_N(\mu, \theta)$ is a random variable drawn from a negative binomial distribution with mean μ and shape factor θ.

To close the lifecycle we assume that the individuals who reproduce in generation $g + 1$ are the survivors of the offspring of generation g, that the expected survival from recruit to spawner is $\widehat{E}$, and that the actual number of spawners is negative binomially distributed around the expected value with shape factor θ_S, so that

$$S_{g+1} = B_N(\widehat{E}R_g, \theta_S). \tag{8}$$

Our first series of experiments uses stock-recruitment functions with a standard Ricker ESR ($R_{max} = 1000$ and $S_{max} = 100$) and expected survival ($\widehat{E} = 0.1$) thus implying a deterministic equilibrium stock of 100 individuals. For each experiment we select values for the process and survival noise (i.e. negative binomial shape factors, θ_R and θ_S), run the model for a 300 generation spin-up period and then generate a 30 year sequence of paired stock and recruitment values.

To simulate the possibility of the fitted model having a potentially different functional form from the true underlying ESR we fit the simulated observations with the eRicker ESR form – which is identical to the sRicker if $k = 1$, but which can also adopt a sigmoidal form (with $k > 1$) or a flatter high-stock shape ($k < 1$). We generate sets of 30 observations with three values of process noise (equivalent to standardised residual standard deviations of 3%, 14% and 32%) and two levels of linear-phase noise (c.v. of 51% and 21%). The resulting fits are shown in Fig. 7 with their quantitative characteristics being given in Table 4.

Table 4: eRicker fits to simulated single population stock recruit data.

θ_R	θ_S	R^2	Resid	R_{max}			S_{max}			k		
			s.d.	2.5%		97.5%	2.5%		97.5%	2.5%		97.5%
10^6	4	0.945	0.038	991	1009	1027	96.6	99.7	103	0.91	1.07	1.11
50	4	0.566	0.15	925	995	1072	93	102	112	0.74	1.03	1.37
10	4	0.238	0.38	889	1089	136880	74	165	10^7	0.21	0.5	1.26
10^6	30	0.762	0.022	996	1006	1016	96	98.3	101	1.02	0.5	1.53
50	30	0.081	0.16	938	991	20559	82	126	3×10^6	0.10	0.58	2.10
10	30	0.21	0.28	1010	1148	5812	110	137	4×10^5	0.25	1.25	2.42

The upper frames in Fig. 7 show experiments with constant θ_S corresponding to realised survivals with a coefficient of variation of approximately 50%. The

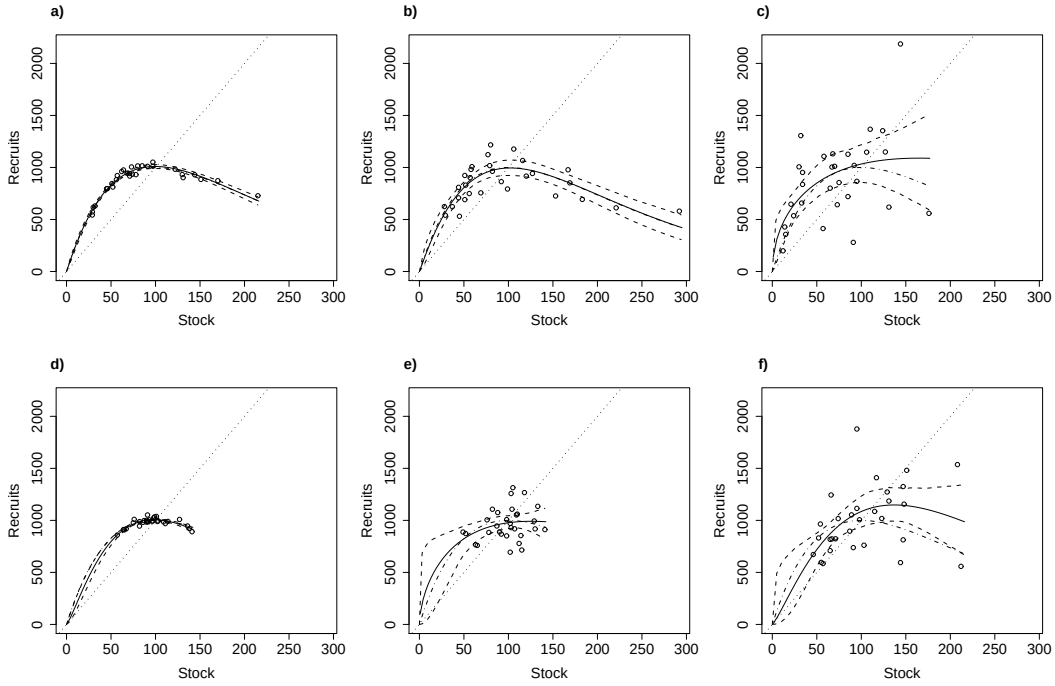

Figure 7: Simulated stock-recruitment observations for a single population with a standard Ricker ESR ($R_{max} = 1000$, $S_{max} = 100$) and expected survival $\widehat{E} = 0.1$. Upper frames (a to c) show increasingly noisy stock recruit functions with survival c.v ≈ 0.5 ($\theta_S = 4$). Lower frames (d to f) show the same stock recruit functions with survival c.v.≈ 0.2 ($\theta_S = 30$). Col 1 (a,d) shows $\theta_R = 1 \times 10^6$ (c.v.$\approx 3\%$). Col 2 (b,e) shows $\theta_R = 50$ (c.v.$\approx 14\%$). Col 3 (c,f) shows $\theta_R = 10$ (c.v.$\approx 32\%$). Points show simulated data. Solid line shows the best fit eRicker ESR, with 95% confidence limits shown by dashed lines. The dash-dotted line shows the true ESR and the dotted straight line is the replacement line.

process noise in the stock-recruitment function varies from a pure Poisson process (c.v.$\approx$3%) in frame a) to $\theta = 10$ (c.v.$\approx$ 33%) in frame c). The lower row of frames show experiments with the same sequence of process noise but survival c.v. $\approx$ 20%.

The right-most columns of Table 4 give the parameters of the best fit to the simulated data in large type and the 5% and 97.5% percentiles from the confidence limits calculations in small type. Comparing these fit statistics and the visual fit quality illustrated (Fig. 7) we see that when survival noise is large and process noise small the eRicker form yields a fit entirely consistent with the true sRicker ESR, and parameter values very consistent with those used in the simulations. Survival c.v $\approx$ 50% and medium process noise (c.v. $\approx$ 15%) yields a fit with ESR parameters and residual s.d. very consistent with the underlying ESR and process noise. Very intense process noise (c.v. $\approx$ 33%) makes the parameter determination much less precise and often (as in the example shown) yields a fitted curve with $k < 1$ indicating a data cloud with weak evidence of stock dependence.

The lower row of simulations and fits illustrates a similar sequence of outcomes, except that the reduced survival noise implies that the (simulated) data covers a smaller fraction of the stock-recruitment relation, thus making the task of ESR identification commensurately harder.

We conclude that noise in the linear and non-linear parts of the life cycle has diametrically opposed effects on stock-recruitment identification. Large variability in the linear part is an essential prerequisite for accurate identification, while process noise in the non-linear part operates in a more intuitive way to reduce our ability to identify the shape of the expected stock-recruitment curve. However, even when the high process noise and short data run cause the fitting process to mis-identify the ESR, the s.d. of the standardised residuals provides an acceptable measure of process noise intensity.

We have repeated these experiments (not shown) with both longer and shorter simulated data sequences. Exactly as one would expect, very short data sequences make the identification task progressively harder, with sequences of less than 10 points being essentially useless for this purpose. Conversely longer sequences make matters much easier, although even a very long sequence will not compensate for a very small range of stock values unless the process noise in the function being sought is extremely small.

Two functionally identical sub-populations

In the last section we saw that while strong year to year variability in the linear portion of the life cycle is a neccesary precondition for stock-recruitment function identification, process noise in the function itself can render such identification problematical. In this section we investigate the effects of analysing observations in which independent sub-populations are regarded as a single unit. As before we assume that the sub-populations have a standard Ricker ESR and negative binomial process noise, so their dynamics are specified by equations (7) and (8).

In our first series of numerical experiments (Fig. 8 and Table 5) we explore a situtation in which two indentical, but statistically independent sub-populations ($R_{max} = 15000$, $S_{max} = 250$, $\widehat{E} = 0.02$) are analysed as a unit. We contrast two realisations of this situation, one in which the linear-phase (normally, but not exclusively, marine) survivals for the two sub-populations are uncorrelated and the other in which they are identical, with the observations which would result if the assessment unit were, in fact, a single population with $R_{max} = 30000$, $S_{max} = 500$, $\widehat{E} = 0.02$. In order to distinguish multiple-subpopulation effects from the effects of short runs of data, we generate sets of simulated observations containing a thousand points.

The first set of experiments concerns component populations with low process noise stock-recruitment relations ($\theta_R = 10^6$) and highly variable linear-phase survival ($\theta_S = 6$). For a single sub-population, we accurately recover the underlying population parameters and the ESR explains a high proportion of the generation to generation variation ($R^2 = 0.996$). Slightly more surprisingly, an

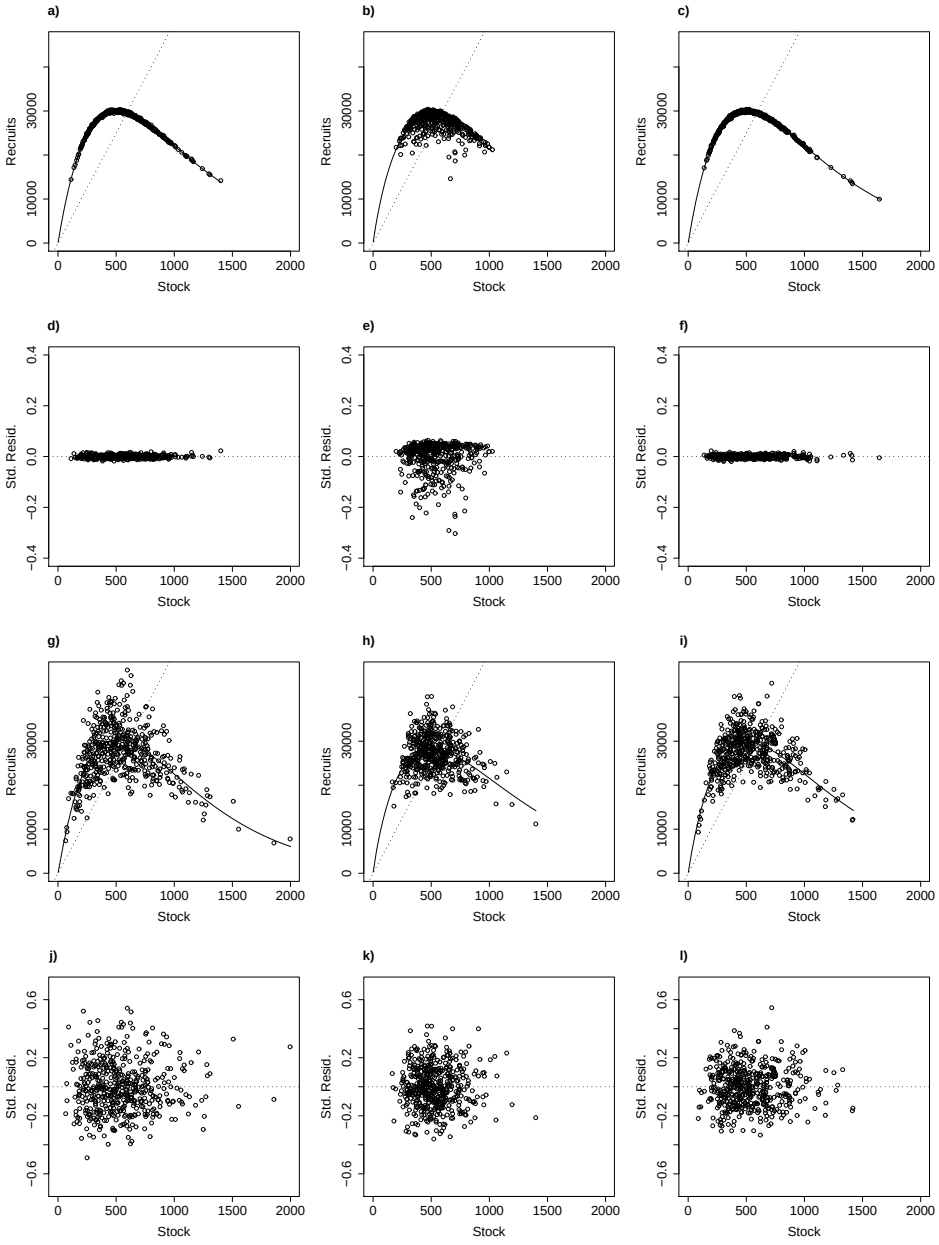

Figure 8: Long-run stock-recruitment simulations for mixed and unitary populations. All have have 1000 observations on a population with sRicker ESR, $\widehat{E} = 0.02$ and highly variable linear-phase survival ($\theta_S = 6 \Leftrightarrow$ c.v.=0.41). Col 1 (a,d,g,j) shows a unitary population with $R_{max} = 30000, S_{max} = 500$. Cols 2 and 3 show populations with two components, each with $R_{max} = 15000, S_{max} = 250$. In Col 2 the sub-populations have independent stock recruitment noise and independent linear-phase survivals. In Col 3, linear-phase survivals are completely correlated. Top two rows (a to f) shows results with pure Poisson stock-recruitment noise ($\theta_R = 1 \times 10^6 \Leftrightarrow$ c.v. $= 0.006$). Lower two rows (g to l) shows results with moderate stock-recruitment noise ($\theta_R = 30 \Leftrightarrow$ c.v.=0.18).

Table 5: Simulated long-series stock-recruitment data for unitary and multiple populations.

Simulation			Fit					Survival
R_{max}	S_{max}	CV_R	R_{max}	S_{max}	k	CV_R	R^2	Correlation
30000	500	0.006	29996	500	1.003	0.006	0.996	–
2×15000	2×250	0.008	28614	495	0.93	0.06	0.451	No
2×15000	2×250	0.008	29992	500	1.004	0.006	0.997	Yes
30000	500	0.18	30355	509	1.03	0.18	0.417	–
2×15000	2×250	0.18	28345	502	0.90	0.14	0.175	No
2×15000	2×250	0.18	29786	511	0.97	0.14	0.416	Yes

essentially similar situation obtains when the assessment unit comprises two sub-populations with identical linear-phase survival; although the recovered parameters are now the sum of the two sub-populations.

When the assessment unit contains two independent sub-populations, although our fit still recovers a parameter set very close to the sum of the two components, the ESR now only explains 45% of the generation on generation variation and the apparent process noise has a c.v. six times as big as that for the component sub-populations (despite their fluctuations being uncorrelated !). The explanation is that uncorrelated variations in the two sub-stocks mean that the per-capita contribution of individuals in one sub-stock can be very different from that in the other – a mechanism also responsible for the biassed residuals (Fig. 8e). When the sub-population stock recruitment relations are themselves noisy, the noise generating effects of uncorrelated sub-stock fluctuations are less spectacular, but are never the less clearly vsible in the low R^2 value implied by Fig. 8h as compared with that in Fig. 8g and Fig. 8i.

Two distinct sub-populations

In view of the clear potential for uncorrelated sub-stock fluctuations to produce apparent process noise even when the sub-stocks have noise-free stock-recruitment relations, our next numerical experiments (Fig. 9 and Table 6) examine sets of simulated observations in which the assessment unit contains sub-populations with distinct characteristics. In these experiments one sub-population has high productivity ($R_{max} = 15000$, $S_{max} = 250$) and low survival ($\widehat{E} = 0.02$) while the other has low productivity ($R_{max} = 7500$, $S_{max} = 250$) and expected survivals in the range $0.04 \rightarrow 0.1$. In all cases the linear-phase survivals of the two sub-populations are uncorrelated.

In the first series of experiments (Fig. 9a to f) the stock recruitment relations of the component populations have very low process noise. In the first experiment (Fig. 9a) the two populations have deterministic equilibria (the point at which the replacement line and the ESR intersect) at the peak of the ESR and their stock-recruitment responses are thus in proportion to their abundance in the

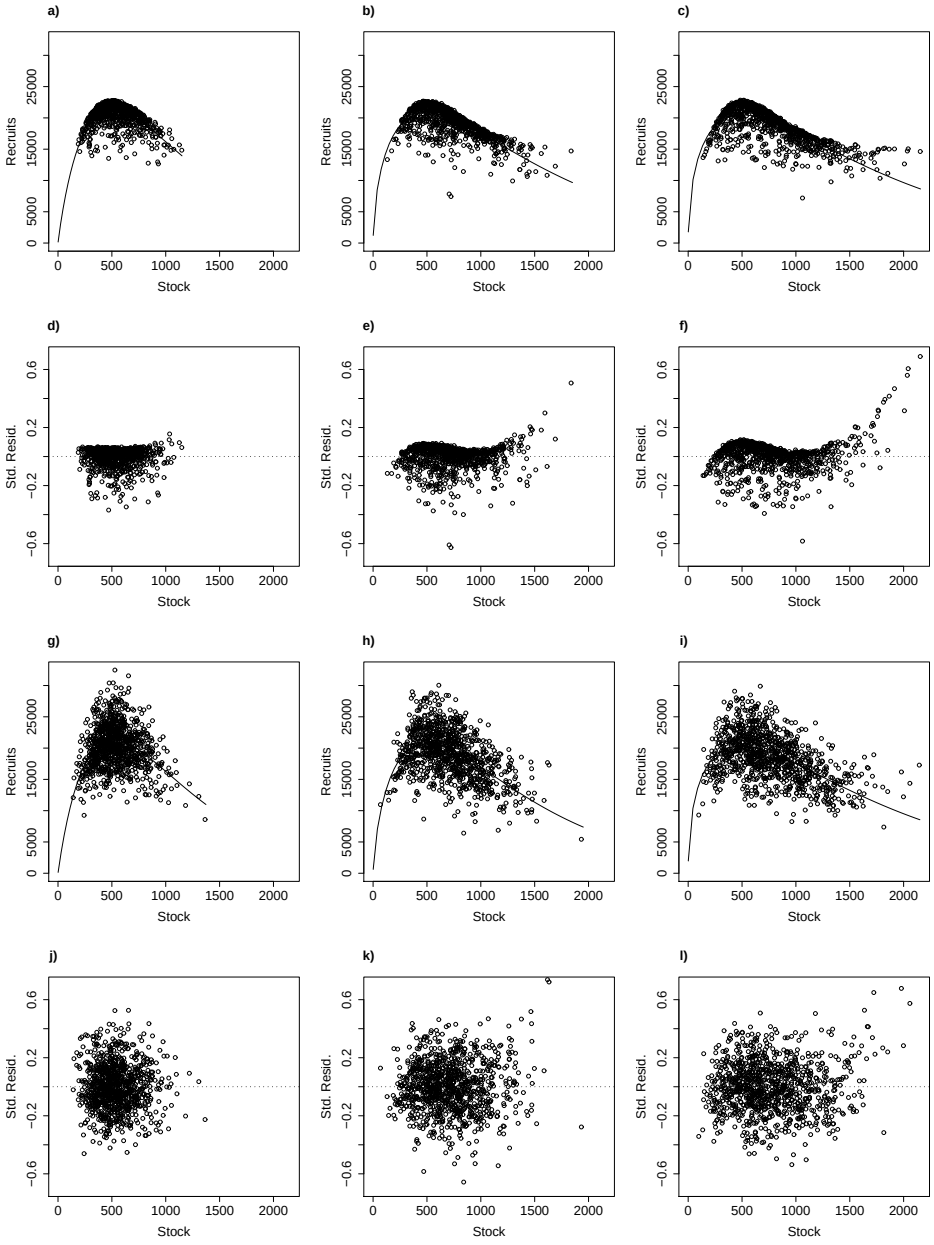

Figure 9: Long-run stock-recruitment simulations for mixed populations with distinct properties. All have have 1000 observations on two populations with sRicker ESR ($R_{max} = 15000$,$S_{max} = 250$ and $R_{max} = 7500$, $S_{max} = 250$ respectively) and highly variable linear-phase survival ($\theta_S = 6 \Leftrightarrow$ c.v.=0.41) uncorrelated between the two sub-populations. Col 1 (a,d.g,j) shows results when expected survivals, $\widehat{E}$, for the more and less productive sub-populations are 0.02 and 0.04 respectively. Col 2 has $\widehat{E} = 0.02$ and 0.08 respectively. Col 3 has $\widehat{E} = 0.02$ and 0.1 respectively. Rows 1 and 2 (a to f) show results for Poisson stock-recruitment noise ($\theta_R = 10^6$) while rows 3 and 4 show results with moderate stock-recruitment noise ($\theta_R = 30 \Leftrightarrow$ c.v.=0.18).

Table 6: Simulated long-series stock-recruitment data for population comprising two sub-populations with sRicker ESR's, one with $R_{max} = 15000$, $S_{max} = 250$ and the other with $R_{max} = 7500$, $S_{max} = 250$..

Simulation			Fit				
$\widehat{E}_1$	$\widehat{E}_2$	CV_R	R_{max}	S_{max}	k	CV_R	R^2
0.02	0.04	0.01	21476	502	0.93	0.07	0.44
0.02	0.08	0.01	20815	497	0.54	0.09	0.54
0.02	0.1	0.01	20472	501	0.47	0.10	0.55
0.02	0.04	0.18	21310	514	0.96	0.17	0.17
0.02	0.08	0.18	20832	500	0.67	0.17	0.30
0.02	0.1	0.18	20323	488	0.45	0.18	0.28

combined population. In this case we see pseudo process noise very comparable to that in Fig. 8b.

However, as we increase the survival of the low-productivity population, thus moving its deterministic equilibrium onto the falling portion of the Ricker curve, we see a considerable increase in the CV of the pseudo process noise, as well as a spectacular increase in the asymetry of the process noise distribution (Figs. 9e and f). Accompanying these changes is a clear alteration in the shape of the composite stock-recruitment relation (Figs. 9b and c), reflected in changes in the fitted k towards values implying a slower decline at high stocks. Interestingly, the R^2 for the fits is somewhat higher for the cases with higher pseudo process noise – because in these cases the range of combined stocks generated by the simulation is increased.

As before, this pattern is largely maintained when the component stock-recruitment relations have significant process noise. We conclude that the combination of an alteration in shape towards less high-stock reduction in recruitment, accompanied by increased process noise flowing from uncorrelated sub-stock variability will make stock-recruitment function identification from feasible sets of composite observations, which seldom exceed 50 years in length, extremely problematical.

Discussion

Sigmoidality and the probability of extinction

Earlier in this paper we showed that several sets of stock-recruitment observations for Atlantic salmon, for example the Girnock ova-fry data, show evidence of sigmoidality (positive curvature at low stock). Further datasets are either compatible with such sigmoidality (River Bush), or define the ESR so poorly that sigmoidality cannot be ruled out (N.Esk). While the low stock ESR has little influence on the mean abundance of a reasonably viable population – essentially the crossing point of the replacement line and the ESR – it can have a pro-

found influence on the time to extinction, and hence on successful conservation of endangered stocks (Fig. 10).

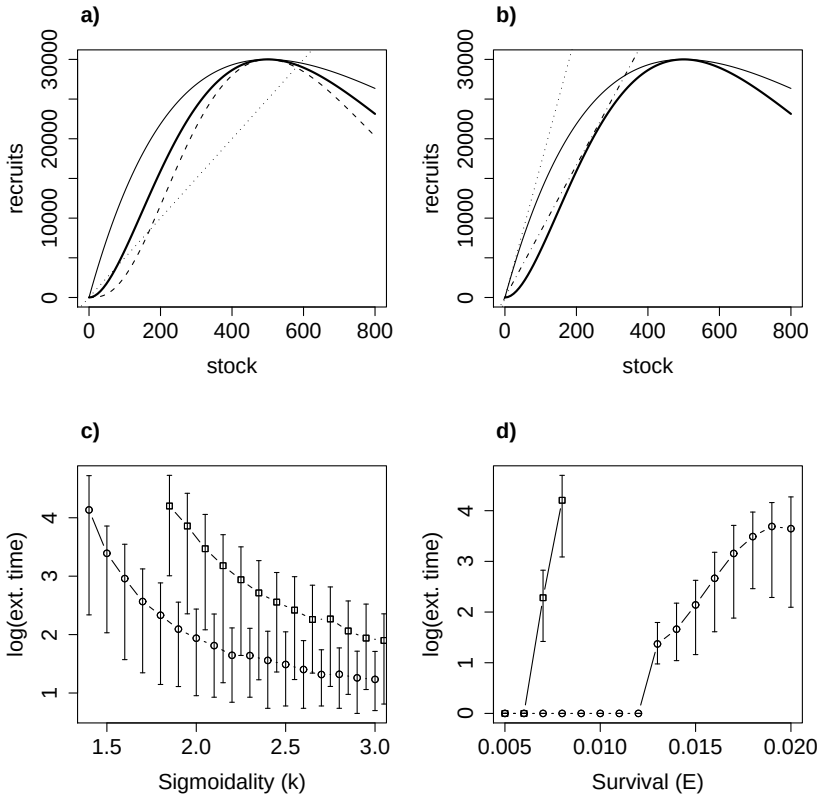

Figure 10: Times to extinction and deterministic dynamics a) shows eRicker ESR curves with $R_{max} = 30000$, $S_{max} = 500$ and $k = 1$(light), 2(heavy) and 3(dashed) compared to the replacement line for $E = 0.02$(dotted). b) shows eRicker ESR curves with $R_{max} = 30000$, $S_{max} = 500$ and $k = 1$(light) and 2(heavy) compared to the replacement lines for $E = 0.006$(dotted) and $E = 0.012$(dashed). c) and d) show mean times to extinction (points) with 2.5 and 97.5 percentiles shown by error bars. In all cases the system had an eRicker ESR with $R_{max} = 30000$ and $S_{max} = 500$ and process noise characterised by $theta_R = 30$ (c.v.≈18%). In c) all runs have $E = 0.02$. Circles show points for $\theta_S = 6$ (c.v.≈41%) and squares for $\theta_S = 20$(c.v.≈22%). In d) all runs have $\theta_S = 20$. Circles show points for $k = 1$ and squares for $k = 2$.

We can see why this occurs by noting that, provided the expected linear-phase survival ($\widehat{E}$) exceeds a threshold value, a sigmoidal ESR crosses the replacement line three times compared to the two crossings for a non-sigmoidal ESR (Fig. 10a). In the non-sigmoidal case the crossing at zero stock is a deterministically repelling steady state (that is any small, positive deviation from it grows) while the interior crossing is deterministically attracting (small deviations decay over time). In the sigmoidal case the zero stock and the high stock crossings are both deterministic attractors and the intermediate crossing is a deterministic

repeller. The intermediate crossing is a thus threshold below which the deterministic dynamics lead inexorably to extinction. We note from Fig. 10a that as an ESR with constant peak height and position becomes more sigmoidal this threshold moves closer to the upper deterministic steady state.

Although the dynamics of our stochastic model are potentially more subtle, we might infer from the above discussion that a stochastic stock-recruitment driven population model might exhibit extinction properties which depend strongly on the low-stock shape of the ESR. In Fig. 10c we see that this expectation is correct. The high noise case shows a time to extinction which drops four orders of magnitude as k is increased from 1.5 to 3. The same trend is visible in the medium noise case albeit with longer extinction times. We note that with these noise levels the time to extinction with $k = 1$ is essentially infinite (that is to say so long that we cannot compute it accurately).

In a related way, the low-stock shape of the ESR has a profund influence on the minimum expected linear phase survival probability at which a population is viable, as we show in Fig. 10b and d. Part of this effect is simply the change in the deterministic survival threshold (the value below which the replacement line crosses the ESR only at the origin). However, although extinction time climbs very steeply away from this threshol in the standard Ricker case ($k = 1$), the sigmoidal case shows a much slower increase and remains vulnerable to extinction for a range of linear-phase survivals which are deterministically viable.

Finally we note a further subtle effect of ESR shape, this time at high stocks. For the sigmoidal case we observe that, for values of $\widehat{E}$ exceeding the deterministic threshold ($\widehat{E} = 0.012$), extinction time at first rises with increasing survival and then appears to pass through a maximum value (just below $\widehat{E} = 0.02$). Continuing the extinction evaluation to even larger survival values (not shown) reveals that beyond $\widehat{E} = 0.02$ extinction time falls with increasing $\widehat{E}$ and eventually becomes very small. As noted by Ripa and Lundberg (2000) this effect occurs with all Ricker-type ESR curves and is driven by their asymptotic approach to zero as S becomes large. Clearly, this effect will not occur if a sigmoidal ESR curve is represented by an extended Beverton-Holt form (equation 2).

Lifecycle partitioning, multiple sub-populations and system identification

The datasets analysed in this paper show that for Atlantic salmon a wide range of choices exists for both the 'stock' and 'recruitment' component of a putative stock-recruitment relation. Pre-fishery adults, total spawners, female spawners, ova, fry and smolts can all, in principle, fullfil either role. For management purposes the most straightforward scheme is to choose a stock measure directly related the viability of the fishery, such as ova or spawning population, and a recruitment measure which has the property that all the non-linear effects (compensation or depensation) occur earlier in the life-cycle than 'recruitment' so the life-cycle closure is linear and the next stock estimate is proportional to recruitment.

For the Girnock Burn population, we have demonstrated that independent non-linear effects occur in the transition from ova to fry and from fry to smolts. We have also demonstrated a complete absence of non-linear effects between emigration to sea and return to the river to spawn. Although we have formally demonstrated this latter effect only for a single component of a catchment population it seems intuitively obvious that it must be a generic property. Thus a pragmatic choice of roles would seem to be ova or spawning population as 'stock' and emigrating smolts as 'recruits'.

Measuring the output of smolts attributable to a single year's spawning activity requires not only the estimation of numbers of smolts emigrating every year, but also the ageing of those emigrants so that they can be attributed to the various spawning years from which they originate. Hence, a superficially appealing alternative choice is to use spawning stock as both stock and recruits, thus ensuring linearity of closure (by eliminating it altogether) and minimisation of measurement effort. However, this strategy has the effect of adding the (very) noisy process of survival at sea to the process noise inherent in the non-linear part of the process, thus producing a stock recruitment relation with very high levels of process noise. Our simulation studies have shown that high levels of process noise make accurate identification and quantification of both the deterministic and the stochastic parts of the stock-recruitment function problematical.

As discussed by Chaput et al. (2003), a further cause of difficulty in system identification is the possibility that single assessment units contain multiple statistically independent sub-populations with distinct properties – for example a population component dominated by one sea-winter fish being combined with another dominated by multi-seawinter individuals. In agreement with the findings of Frank and Brickman (2000), our simulation studies show that even if the true stock recruitment relations of the two population components are identical, their non-linearity combined with the statistical independence of the component populations can produce significant additional pseudo process noise in the composite stock recruitment relation, thus making its accurate identification difficult. Where the two components have very different properties in either the non-linear or the linear portions of the life-cycle, the composite stock recruitment relation shows low stock dependence, accompanied by intense, highly biassed, process noise, thus making accurate reconstruction all but impossible.

Stock-recruitment observations and policy objectives

In traditional fisheries management practice, the concentration has been on attaining maximum sustainable yield (MSY) – a target which requires knowledge of the shape of the expected stock-recruitment curve at healthy levels of recruitment. However, in many jurisdictions, the response to steadily decreasing numbers of Atlantic salmon has been to shift the emphasis to conservation of potentially endangered stocks – a target which is critically dependent on the

low-stock shape of the expected stock recruitment curve, on the process noise around the ESR and on the levels of noise in the linear phase of the life-cycle.

In this paper we have shown that positive curvature (sigmoidality) in the low-stock portion of the ESR can have profound effects on the viability of a stock. Our examination of a representative selection of the richer stock-recruitment datasets for Atlantic salmon show that a hypothesis of sigmoidality can be ruled out in only a small minority of cases. Thus a prudent choice of ESR function for conservation management use will be a function which is capable of exhibiting this property. Of the two candidate functions with this capability examined in this paper we note that the asymptotic approach of the eRicker to zero recruitment at high stock can dominate estimates of time to extinction. Hence, unless there is clear evidence of such a high-stock decline in production, we believe the extended Beverton-Holt (eBH) form (equation 2) to represent a conservative choice of candidate ESR function.

In this context we note that composite stock-recruitment relations derived from data encompassing a group of disparate quasi-independent sub-populations can exhibit a variety of apparent shapes, which are in addition often very hard to discern amid the excess pseudo process noise such compositing generates. We thus believe that a very high standard of proof would be required before an eRicker form would be a prudent choice of ESR form for conservation management purposes. However, the eRicker form is arguably the most flexible and intutive form to use in the course of data investigation, since its repertoire includes sigmoidal, simple Ricker and essentially stock-independent shapes.

When considering the parameters to use in management evaluations it has been conventional to utilise the best fit parameters for whatever candidate ESR has been chosen. While this strategy arguably yields something close to a maximum likelihood estimate for the maximum sustainable yield, it does not yield a suitably conservative estimate of extinction time for conservation use. To obtain a 'worst-case' estimate of extinction time, one would fit a potentially sigmoidal ESR form and use the lower limit of the ESR confidence envelope for extinction time evaluation. The appropriate confidence level for this envelope clearly depends on the level of risk deemed acceptable. For most purposes 95% confidence would seem a suitable choice, but for particularly valuable or sensitive populations, 99% (or even more) could be needed.

Acknowledgements

The authors gratefully acknowledge the numerous field workers, from many countries, who have amassed the datasets used in this paper.

References

Bacon, P.J., Gurney, W., Jones, W., McLaren, L.S., Youngson, A.F., 2005. Seasonal growth patterns of wild fish: partitioning among explanatory variables

on the basis of individual growth trajectories of Atlantic salmon parr, Journal of Animal Ecology, 74, 1–11.

Beverton R.J.H. and Holt S.J., 1957. On the dynamics of exploited fish populations, U.K. Ministry of Agriculture, Fisheries and Food, Fisheries Investigations (Series 2), 19, 533–.

Chaput G. and Jones R., 1992. Stock-recruitment relationship for multi-sea-winter salmon from the Margaree river, N.S., Fisheries and Oceans Canada, CFSAC Research Document 92/124,,

Chaput G., Crozier W.W., Davidson I.C., Dempson J.B., Erkinaro J., Erikstad L., Fleming I.A., Guobergson G., Hansen L.P., Hindar K., Insulander C., Jensen A.J., Johlander A., Karlsson L., MacLean J.C., Mathers R.G., Milner N.J., Nicholson M.D., O Maoileidigh N., Potter E.C.E., Prevost E., Schon P-J., and Wyatt R.J., 2003. A co-ordinated approach towards the development of a scientific basis for management of wild Atlantic salmon in the North-East Atlantic (SALMODEL), Queens University of Belfast, Belfast, United Kingdom,

Chen D.G. and Irvine J.R., 2001. A semiparametric model to examine stock recruitment relationships incorporating environmental data, Canadian Journal of Fisheries and Aquatic Science, 58, 1178–1186.

Chen D.G., Irvine J.R. and Cass A.J., 2002. Incoporating Allee effects in fish stock-recruitment models and applications for determining reference points, Canadian Journal of Fisheries and Aquatic Science, 59, 242–249.

Chen D.G. and Holtby L.B., 2002. A regional meta-model for stock recruitment analysis using an empirical Baysian approach, Canadian Journal of Fisheries and Aquatic Science, 59, 1503–1514.

Clark C.W., 1990. Mathematical Bioeconomics, John Wiley and Sons, New York, Chichester, Brisbane, Toronto, Singapore,

Crozier W.W. and Kennedy G.J.A., 1995. The relationship between a summer fry (0^+) abundance index derived from semi-quantitative electrofishing and egg deposition of Atlantic salmon, in the River Bush, Northern Ireland, Journal of Fish Biology, 47, 1055–1062.

Davidson A.C. and Hinkley D.V., 1997. Bootstrap Methods and their Application, Cambridge University Press, Cambridge U.K.,

Frank K.T. and Brickman D., 2000. Allee efects and compensatory population dynamics within a stock complex, Canadian Journal of Fisheries and Aquatic Science, 57, 513–517.

Gurney W.S.C., Bacon P.J., Tyldesley G., and Youngson A.F., 2009. Process-based modeling of decadal trends in growth survival and smolting of wildslamon (*Salmon salar*) parr in a Scottish upland stream, Canadian Journal of Fisheries and Aquatic Science, in press, –.

Locke A. and Mowbray F., 1995. Status of Atlantic salmon in the Nepisiguit River, New Brunswick, Fisheries and Oceans Canada, CFSAC Research Document 96/129,,

Michielsens C.G.J. and McAllister M.K., 2003. A Bayesain hierarchical analysis of stock-recruit data: quantifying structural and parameter uncertainties, Canadian Journal of Fisheries and Aquatic Science, 61, 1032–1047.

Myers R.A., Barrowman N.J., Hutchings J.A. and Rosenberg A.A., 1995. Population dynamics of exploited fish stocks at low population levels, Science, 269, 1106–1108.

Myers R.A., 2001. Stock and recruitment: generalizations about maximum reproductive rate, density dependence and variability using meta-analytic approaches, ICES Journal of Marine Science, 58, 937–951.

Needle C.L., 2002. Recruitment models: diagnosis and prognosis, Reviews in Fish Biology and Fisheries, 11, 95–111.

Ripa J. and Lundbery P., 2000. The route to extinction in variable environments, Oikos, 90(1), 89–96.

Ricker W.E., 1954. Stock and recruitment, J. Fish. Res. Board Can., 11, 559–623.

Roughgarden J., Gaines S. and Possingham H., 1988. Recruitment Dynamics in Complex Life Cycles, Science, 241, 1460–1466.

Sakuramoto K., 2005. Does the Ricker or Beverton-Holt type of stock-recruitment relationship truly exist, Fisheries Science, 71, 577–592.

Shearer W.M., 1990. The Atlantic salmon (*Salmo salar*) of the N. Esk with particular reference to the realtionship between sea-age and time of return to home waters, Fisheries Research, 10, 93–123.

Schnute J.T. and Kronlind A.R., 2002. Estimating salmon stock-recruitment relationships from catch and escapement data., Canadian Journal of Fisheries and Aquatic Science, 59, 433–449.

Appendices

A. Fits to simulated Girnock spawner → fry datasets

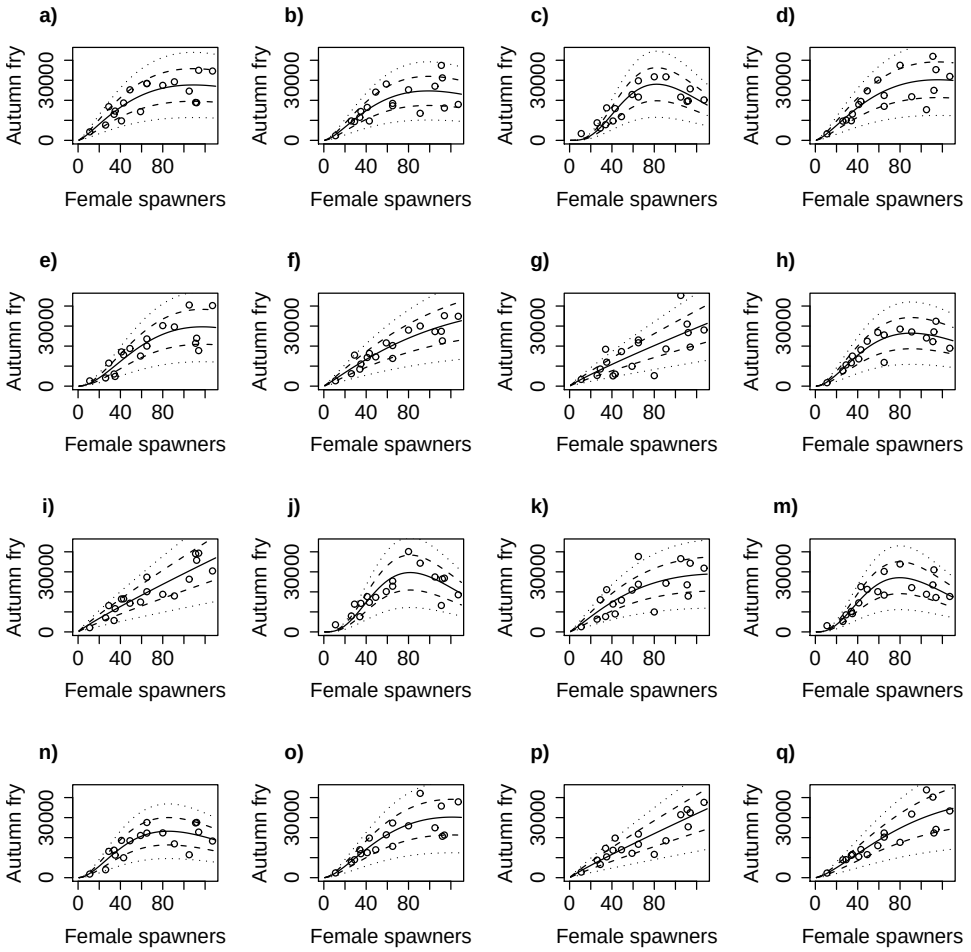

Figure A1: Sixteen example fits of the eRicker model to simulated datasets generated by assuming that recruitment values at the same stock values present in the observations are drawn from a normal distribution with the mean taken from the best fit to the observations (Fig. 1a) and s.d. chosen to make the c.v. of observations at that stock equal to 0.294. a) to q) show fits to datset numbers 62, 124, 186, 248, 310, 372, 434, 496, 558, 620, 682, 744, 806, 868, 930 and 992 respectively out of a series of 1000.